

Classification of Distorted Overlapping Fingerprints with Fuzzy Geometrical Features

Sankar K. Pal Suptendra Nath Sarbadhikari

Machine Intelligence Unit,
Indian Statistical Institute,
Calcutta 700035,
INDIA.

Email: sankar@isical.ernet.in
res9519@isical.ernet.in
Fax: (+91) (33) 5566680

Abstract

Overlapping fingerprints are naturally abundant and pose great difficulty for proper identification. In this article, we demonstrate the effectiveness of fuzzy geometrical features for classifying distorted overlapping fingerprints directly from raw unprocessed images. The input vector consists of some selected fuzzy geometrical features. The output vector is defined in terms of six classes viz., Left-loop, Right-loop, Twin-loop, Plain-arch, Whorl and Overlapping. Overlapping (between any two of the above five pure classes) in various degrees and orientations are artificially produced on pure fingerprint images. Distorted patterns are generated for all the six classes, with random noise, cut marks and information loss in certain random locations. The fuzzy geometrical features viz., length, height and index of area coverage are found to be the best for classifying these patterns when Bayes', k -NN (with $k = 1, 3, 5$) and MLP (multi-layer perceptron) classifiers are used. The overall performance is best for MLP, followed by 1-NN. Improvement in recognition scores with the increase in number of training samples is found to be significant for 3-NN rule.

Keywords: Overlapping Fingerprints; Fuzzy Geometrical Features; Pattern Recognition; Multi-layer Perceptron (MLP); k -NN (k nearest neighbor) Classifier; Bayes' Classifier.

1 Introduction

Matching of fingerprints is recognized as a basic tool for positive identification of individuals, be it for criminals in law enforcement, for security clearance in the armed services, or for normal civilian identification purposes. For this process it is necessary to maintain large files of fingerprint records. Automated computer processing promises a fast and accurate alternative in this sphere.

The computer based identification of fingerprints involves two major steps: [1] (a) "preprocessing" like enhancement of images, thresholding (converting gray levels to binary *i.e.*, black and white), thinning of ridges (black concentric lines), and extraction of features (b) Classification and analysis of the processed (quality enhanced) image. Fingerprints are identified in a hierarchical manner. The preprocessed (binary) images are classified, by determining different micro characteristic features like ridge flow and minutiae type, number and position. Multilevel classifier based on syntactic approach [2], graph matching [3], detecting the number and locations of singular points [4] and minutiae features [1], after smoothing the binary images have been tried for classification of fingerprints. Recently neural networks are being used for this purpose. Artificial neural networks (ANN) [5] can be formally defined as a *massively parallel interconnected network of simple (usually adaptive) processing elements that interact with objects of the real world in a manner similar to biological systems*. The benefit of neural nets lies in the high computation rate provided by their inherent massive parallelism, thereby enabling real-time processing of huge data sets with proper hardware backing. The networks are also found to be robust to input noise and generally degrade gracefully to loss of components. Various methods using networks for classification of

binary ridge patterns for each fingerprint category have been developed [6, 7, 8].

One may note that using binary images, in all the above techniques, often leads to information loss in the final decision making process. Moreover, it is not appropriate to commit oneself to a specific thresholding for binarization particularly when the ridges are not well defined. For example, in the case of forensic applications, the quality of fingerprint data is often found to be very poor because of the faint nature, noise and incompleteness. The conventional preprocessing techniques based on heuristic logic are usually incapable of handling such situations, often leading to erroneous processed results at the cost of expensive computer time. So, it is desirable to have a system where such time consuming and error prone preprocessing techniques could be altogether avoided.

By computing input features directly from the raw fingerprints, the uncertainties in reaching a decision and also the overall computational burden are greatly reduced [9, 10]. Based on this realization, Pal and Mitra [11] computed fuzzy geometrical features and probabilistic entropy measures directly from unprocessed fingerprint images for their classification using multilayer perceptron (MLP). There is another investigation on fingerprint classification using fuzzy MLP [12] where it exploits the nonlinear boundary generating capability of MLP and the uncertainty handling capacity of fuzzy sets for providing a more intelligent system. Note that fuzzy geometrical features are found to be useful for various image processing problems [13, 9, 10].

Again, in real life, overlapping fingerprints are quite abundant and pose great difficulty in proper identification. Sometimes, for example in forensic investigations, an overlapping fingerprint has got greater significance and requires special attention. Moreover, the overlapping fingerprints - like the

pure ones - are also liable to be corrupted by distortions. Hence, overlapping fingerprints need to be identified even in the presence of extraneous corruptions.

The present article is an attempt at developing a methodology for noisy and distorted overlapping fingerprint classification, exploiting the characteristics of fuzzy geometrical features, derived from the gray images, as input. Here we consider overlapping fingerprints as a separate class. Different percentages (*e.g.*, 25%, 50%, 75%) of overlapping in various orientations between the separate fingerprint classes (*e.g.*, left-loop, right-loop, twin-loop, plain arch and whorl) are considered. The performance of a standard classifier, like, the MLP, in the presence of different types of distortions (*e.g.*, random noise, cut-mark, smudging, under-inking and averaging) is studied. The network's performance is compared with that of the k-NN classifier and Bayes' classifier. The investigation also finds the best set of fuzzy geometrical features for providing the highest recognition scores and the variation of recognition scores with the size of training data.

Section 2 describes the various pure fingerprint classes, overlapping fingerprint generation procedure and the method of fuzzy geometrical feature extraction. This is followed by an outline of the various classifiers used, in Section 3. Section 4 presents the way of implementation and results. Conclusions are drawn in Section 5.

2 Fingerprint Categories and Fuzzy Geometrical Features

2.1 Fingerprint categories

Fingerprint images essentially consist of two types of characteristic regions, *viz.*, ridges and valleys. These ridges run somewhat parallelly and slowly over the finger. The ridge structure and the skin texture provide the uniqueness to the fingerprint, and this remains unchanged during one's lifetime. A fingerprint consists of three regions, *viz.*, core area, marginal area and base area. The ridges from these three areas meet at a triangular formation called the delta region. The centroid of this region is identified as the delta point.

Depending upon the ridge flow on the core area and the number of delta points, fingerprints can be broadly classified (according to Henry) [14] as

- Loop : This is the most common type. Ridges enter from one side, proceed towards the center and then turn to leave from the same side. There are two common categories, *viz.*, Left Loop and Right Loop, depending on the direction of the loop formed. In a third variety, Twin or Double Loop, the core area consists of ridges from two distinct loop patterns.
- Arch : In Plain Arch, ridges enter from one side, rise in the middle and leave on the other side. The Tented Arch is same as the Plain Arch, but the amount of rise in the middle is more here.
- Whorl : Ridge flow in the core area is circular, and two delta points are defined. However, there may be two subtypes, *viz.*, Central Pocket and Elliptical Whorl. In the first

subtype, there are circular ridges in the core, but it becomes asymmetric towards the base, *i.e.*, between whorl and loop. In the other subtype the ridges are stretched in the direction of the finger. The distance between the end points of these stretched ridges are distinct.

- **Accidental or Mixed or Composite :** This type consists of those patterns that cannot be classified under any of the above categories.

In this work, we study the feasibility of our method on five common classes, *viz.*, Left Loop, Right Loop, Twin Loop, Plain Arch and Whorl. Fig. 1 shows some typical images of these five different fingerprint categories. Apart from these five pure classes, we have generated overlapping patterns of fingerprints by superimposing any two of the five classes in various degrees and orientations, as described in the next subsection. In our database, the images are kept at the same scale and approximately with the same orientation. They are 256×256 in size with 8 bits per pixel and labeled manually.

2.2 Overlapping fingerprint generation

For generating an overlapping fingerprint, first of all, an image (background image) is chosen randomly from the five pure classes (*viz.*, left-loop, right-loop, twin-loop, plain-arch and whorl). A second (overlapping) image (belonging to another fingerprint class) is then superimposed on the background image. The resultant superimposed intensity at a point is considered to be the maximum gray value of the corresponding pixels of the two images at that point. For example, in each of the Figs. 2a-c, the background fingerprint image belongs to right-loop class, while the overlapping image is a left-loop. A total of ten types

of overlapping fingerprints thus produced, correspond to 100% overlapping (Fig. 2h), 25% or 50% or 75% overlapping (individually along x or y axis as shown in Figs. 2a-d) and 25% or 50% or 75% overlapping (simultaneously along both the axes as shown in Figs. 2e-g).

2.3 Feature Extraction

A fuzzy subset of a set S is a mapping μ from S into $[0, 1]$. For any $p \in S$, $\mu(p)$ is called the degree of membership of p in μ . A crisp (ordinary or nonfuzzy) subset of S can be regarded as a special case of a fuzzy subset in which the mapping μ is into $\{0, 1\}$. Some of the fuzzy geometrical properties of μ , relevant to the present work, are described below [9, 11].

Let $\mu(I)$ denote a fuzzy representation of an $N_x \times N_y$ image I , *i.e.*, a mapping μ from $I \in \{1, \dots, N_g\}$ into $[0, 1]$ representing a fuzzy subset of I . For convenience, we shall use μ only to denote $\mu(I)$ in this work.

Area : The area of a fuzzy subset μ is defined as

$$a(\mu) = \int \mu \quad (1)$$

where the integration is taken over a region outside which $\mu = 0$. For μ being piece-wise constant (in case of digital image) the area is

$$a(\mu) = \sum \mu, \quad (2)$$

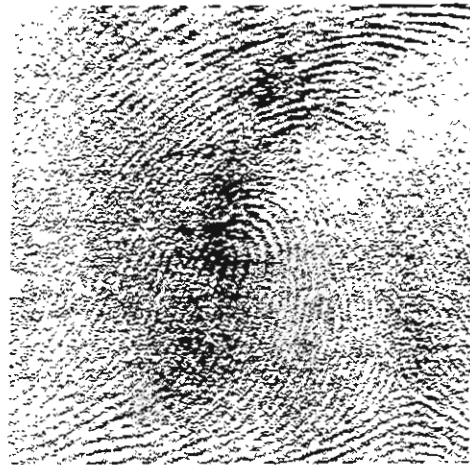
the summation being considered over a region outside which $\mu = 0$. The area is therefore the weighted sum of the regions on which μ has constant value weighted by these values.

Perimeter : If μ is piece-wise constant, the perimeter of μ is defined as

$$p(\mu) = \sum_{i,j,k} |\mu(i) - \mu(j)| \times |A(i, j, k)|. \quad (3)$$



(a) Left Loop



(b) Right Loop



(c) Twin Loop



(d) Plain Arc

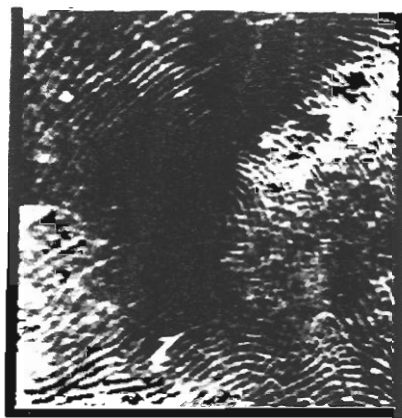


(e) Whorl

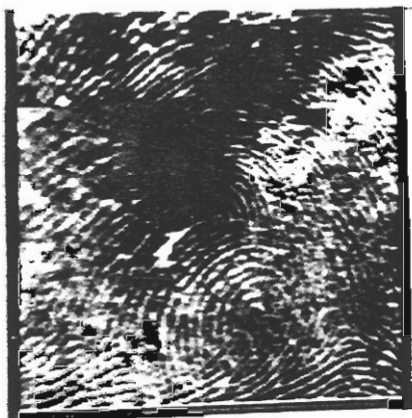
Figure 1 - The five categories of fingerprint patterns



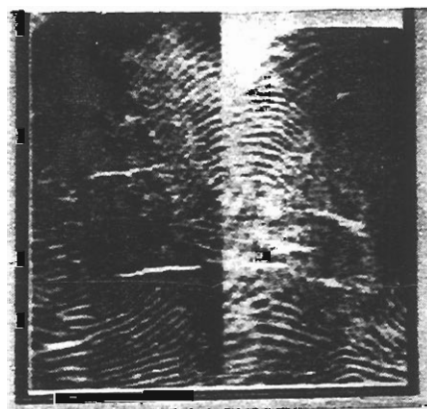
(a) 25% in y-axis



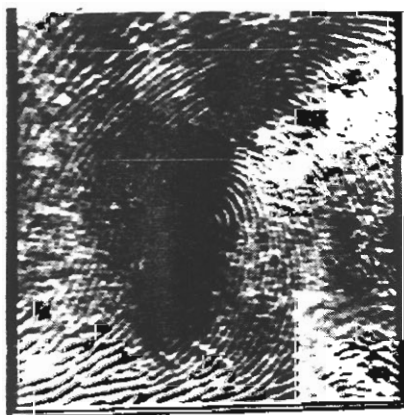
(b) 50% in y-axis



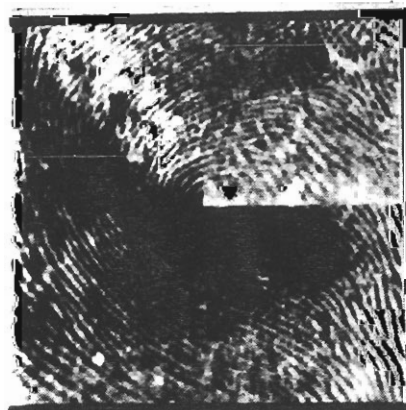
(c) 75% in y-axis



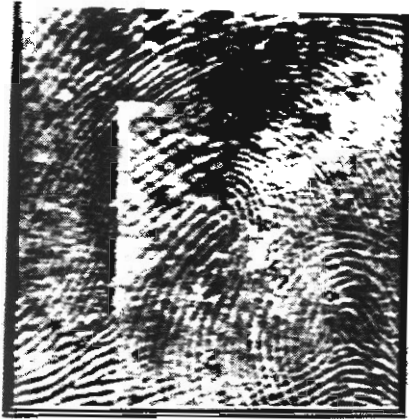
(d) 50% in x-axis



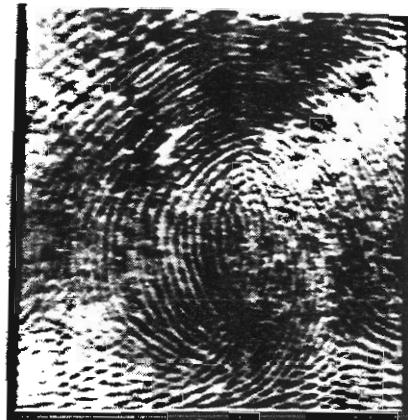
(e) 25% in x-axis + 25% in y-axis



(f) 50% in x-axis + 50% in y-axis



(g) 75% in x-axis + 75% in y-axis



(h) 100% total overlapping

Figure 2 - Different types of overlapping fingerprint patterns

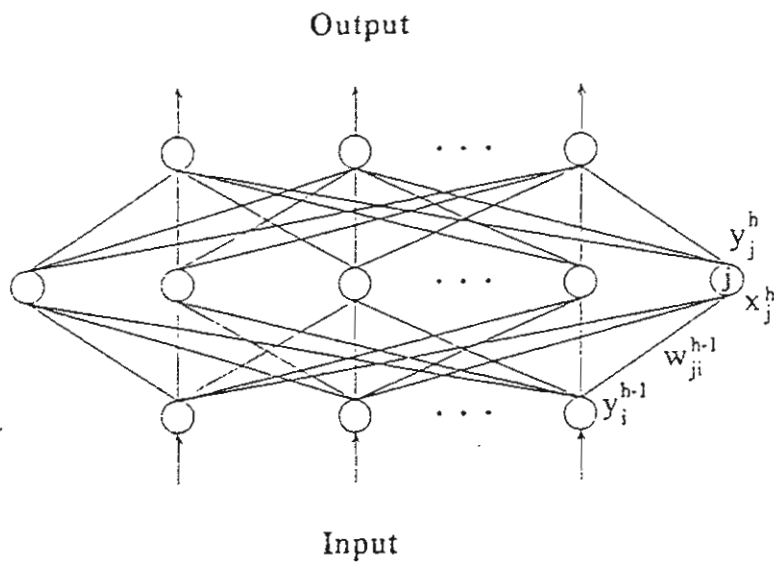


Fig. 3. The three-layered MLP model.

This is just the weighted sum of the lengths of the arcs $A(i, j, k)$ along which the regions having μ values $\mu(i)$ and $\mu(j)$ meet, weighted by the absolute difference of these values. In case of an image if we consider the pixels as the piece-wise constant regions, and the common arc length for adjacent pixels as unity then the perimeter of an image is defined by

$$p(\mu) = \sum_{i,j} |\mu(i) - \mu(j)| \quad (4)$$

where $\mu(i)$ and $\mu(j)$ are the membership values of two adjacent pixels.

Compactness : The compactness of a fuzzy set μ having area $a(\mu)$ and perimeter $p(\mu)$ is defined as

$$comp(\mu) = \frac{a(\mu)}{p^2(\mu)} \quad (5)$$

Physically, compactness means the fraction of maximum area (that can be encircled by the perimeter) actually occupied by the fuzzy region/concept represented by μ .

Height and Width : The height $h(\mu)$ and width $w(\mu)$ of a fuzzy set μ are defined as

$$h(\mu) = \int \max_x \{\mu(x, y)\} dy \quad (6)$$

and

$$w(\mu) = \int \max_y \{\mu(x, y)\} dx \quad (7)$$

where the integration is taken over a region outside which $\mu(x, y) = 0$. For a digital picture the definitions take the form

$$h(\mu) = \sum_y \max_x \{\mu(x, y)\} \quad (8)$$

and

$$w(\mu) = \sum_x \max_y \{\mu(x, y)\} \quad (9)$$

So, height (width) of a digital picture is the sum of the maximum membership values of each row (column).

Length : The length of a fuzzy set μ may be defined as

$$l(\mu) = \max_x \left\{ \int \mu(x, y) dy \right\} \quad (10)$$

where the integration is taken over the region outside which $\mu(x, y) = 0$. In case of a digital picture the expression takes the form

$$l(\mu) = \max_x \left\{ \sum_y \mu(x, y) \right\} \quad (11)$$

Breadth : The breadth of a fuzzy set μ may be defined as

$$b(\mu) = \max_y \left\{ \int \mu(x, y) dx \right\} \quad (12)$$

where the integration is taken over the region outside which $\mu(x, y) = 0$. For a digital image

$$b(\mu) = \max_y \left\{ \sum_x \mu(x, y) \right\} \quad (13)$$

The length (breadth) of an image fuzzy subset gives its longest expansion in the y direction (x direction). If μ is crisp, $\mu(x, y) = 0$ or 1 ; then length (breadth) is the maximum number of pixels in a column (row).

Index of Area Coverage (IOAC) : The index of area coverage of a fuzzy set may be defined as

$$IOAC(\mu) = \frac{a(\mu)}{l(\mu) \times b(\mu)} \quad (14)$$

IOAC of a fuzzy image subset represents the fraction (which may be improper also) of the maximum area (that can be covered by the length and breadth of the image) actually occupied by the image.

3 Classifiers used

3.1 MLP based model

The multilayer perceptron (MLP) [5] consists of multiple layers of simple, two-state, sigmoid processing elements (nodes) or neurons that interact

using weighted connections. After a lowermost input layer there are usually any number of intermediate or *hidden* layers followed by an output layer at the top. There exist no interconnections within a layer while all neurons in a layer are fully connected to neurons in adjacent layers. Weights measure the degree of correlation between the activity levels of neurons that they connect.

An external input vector is supplied to the network by clamping it at the nodes in the input layer. For conventional classification problems, during training, the appropriate output node is clamped to state 1 while the others are clamped to state 0. This is the desired output supplied by the *teacher*.

Consider the network given in Fig. 3. The total input x_j^{h+1} received by neuron j in layer $h+1$ is defined as

$$x_j^{h+1} = \sum_i y_i^h w_{ji}^h - \theta_j^{h+1} \quad (15)$$

where y_i^h is the state of the i^{th} neuron in the preceding h^{th} layer, w_{ji}^h is the weight of the connection from the i^{th} neuron in layer h to the j^{th} neuron in layer $h+1$ and θ_j^{h+1} is the threshold of the j^{th} neuron in layer $h+1$.

The output of a neuron in any layer other than the input layer ($h > 0$) is a monotonic non-linear function of its total input and is given as

$$y_j^h = \frac{1}{1 + e^{-x_j^h}} \quad (16)$$

The Least Mean Square (LMS) error in output vectors, for a given network weight vector w , is defined as

$$E(w) = \frac{1}{2} \sum_{j,c} (y_{j,c}^H(w) - d_{j,c})^2 \quad (17)$$

where $y_{j,c}^H(w)$ is the state obtained for output node j in layer H in input-output case c and $d_{j,c}$ is its desired state specified by the teacher.

One method for minimization of $E(w)$ is to apply the method of gradient-descent by starting with any set of weights and repeatedly updating each weight by an amount

$$\Delta w_{ji}^h(t) = -\epsilon \frac{\partial E}{\partial w_{ji}^h} + \alpha \Delta w_{ji}^h(t-1) \quad (18)$$

where the positive constant ϵ controls the descent, $0 \leq \alpha \leq 1$ is the damping coefficient or momentum, and t denotes the number of the iteration currently in progress.

After a number of sweeps through the training data, the error $E(w)$ in eqn. (17) may be minimized. At this stage the network is supposed to have discovered (learned) the relationship between the input and output vectors in the training samples.

A three layered MLP (multi-layer perceptron) [5] (Fig. 3), with suitably chosen architecture, is used for classifying the fingerprint patterns. It accepts the fuzzy geometrical features as input, and produces output signifying the presence of some particular class. The number of output nodes is equal to the number of fingerprint categories to be classified, i.e., six (e.g., left-loop, right-loop, twin-loop, plain arch, whorl and overlapping) in the present case. The number of input nodes and nodes in the hidden layer are varied according to the number of fuzzy geometrical features used as input.

3.2 *k*-nearest neighbor classifier

The *k*-NN classifier is reputed to be able to generate piecewise linear decision boundaries and, thereby, is quite efficient in handling concave and linearly nonseparable pattern classes. Therefore, a comparison of the performance of the MLP model with that of the *k*-NN classifier is highly appropriate. The *k*-NN classifier is practical when large amounts of memory and sufficient computa-

tion power are available for a rapid single trial learning. For purveying good generalization, the distance between stored exemplar and input patterns is computed by Euclidean distance metrics E as:

$$E_{i,j} = \sum_{d=1}^D |T_d^i - U_d^j|$$

where D is the dimension of the feature vectors, T^i is the i th test vector and U^j is the j th training vector.

3.3 Bayes' classifier

Here, the Bayes' classifier with multivariate normal class conditional densities and *a priori* class occurrence probabilities $p_i = |C_i|/N$ has been used. Here C_i indicates the number of patterns in the i th class and N is the total number of pattern points. The covariance matrices for the pattern classes are considered to be different.

4 Implementation and Results

4.1 Obtaining the pure and distorted fingerprint images

We had originally altogether 50 samples comprising five different types of patterns. With an objective of testing the effectiveness of the method, in the presence of distorted images, we generate 250 more patterns by introducing distortions (*e.g.*, random noise, cut-mark, smudging and under-inking) into the pure fingerprint patterns. From the 50 pure samples, we randomly choose two fingerprint patterns belonging to two separate classes and superimpose them in various degrees and orientations for producing ten types of overlapping patterns, as described in Sec-

tion 2.2. In this way, with different original images (a total of ten combinations) we have a total of 100 overlapping images. We also introduce the five varieties of distortions described in each of the 100 overlapping images to produce 500 distorted overlapping images. The ways of introducing various types of distortions are described below.

4.1.1 Random noise generation

A predefined percentage (10) of pixels are selected and random noise is injected in the corresponding gray values. Let the magnitude of noise so added be represented by $X = x$, where X is normally distributed. We use $X \sim N(m, \sigma)$, where m is the mean and σ is the standard deviation of the normal distribution. Thus, if a pixel p with gray value G_p is selected randomly, its new gray value becomes $G_p = G_p + x$, such that $0 < G_p \leq N_g$ (Figure 4).

4.1.2 Cut mark

Any two points in the fingerprint image are selected randomly and the pixels lying on a width b_w joining these two points are set to the highest gray value, N_g . That is, $G_p = N_g$ was used for all pixels p lying along the generated line (of width b_w), to simulate a cut mark on the fingerprint image. The cutmarks are generated in two different orientations (along the first and second diagonals of the image), at 90° difference. These are termed as the *forward* and *reverse* directions respectively (Figure 4).

4.1.3 Missing information

To model the occurrence of loss of information in some portion of the fingerprint image, we select a portion of the image randomly. Setting all pixels within this portion to the highest (N_g) or lowest

(1) gray value simulates the loss of information in that region. So, $G_p = N_g(1)$ for all pixels p lying within the randomly selected part of the image. Note that, setting $G_p = N_g$ models the case for insufficient inking (information loss - white) of the fingerprint in the concerned region, while, setting $G_p = 1$ simulates the condition of excess inking (information loss - black) or blotches or smudging (Figure 4).

4.1.4 Averaging

We randomly select several seed points and generate boxes of size $b_s \times b_s$ around these points in each case. Then the gray values of the pixels within these regions are replaced by the average of all pixels within the respective boxes.

4.2 Net parameters

The MLP based classification scheme is subjected to on-line learning using standard back propagation algorithm. The thresholds of all neurons are set to zero. The following architecture is selected empirically. There are altogether three layers (one hidden layer). Out of the eight fuzzy geometrical features described in Section 2.3, various combinations of seven features (excluding area - which is not significantly different for the different classes) are used as input. Either three (height + length + IOAC; or width + breadth + IOAC or perimeter + compactness + IOAC) or four (height + length + width + breadth) or five (height + length + perimeter + compactness + IOAC) features are taken together. The input layer has 3, 4 or 5 nodes in accordance with the number of fuzzy geometrical features used as input. The hidden layer consists of 3 nodes. The output layer, consisting of six nodes corresponding to six different classes (e.g., left-loop, right-loop, twin-loop, plain arch, whorl and overlapping), is fully connected to the

hidden layer.

4.3 Training and testing

The experiment consists of eleven parts as shown in Table 1. For example, in part 1, we consider ten (pure) images from each of the five pure fingerprint classes (*viz.*, left-loop, right-loop, twin-loop, plain arch and whorl) and ten images from 25% overlapping class, *i.e.*, a total of sixty fingerprint images as training patterns. Similarly, in parts 2 to 10, we consider the other nine types of overlapping fingerprint images, keeping the fifty pure fingerprint images the same. In part 11, ten images (one from each of the ten types of overlapping) are considered to form the set of overlapping fingerprint images as training samples. Here also, the same fifty pure fingerprint images are used.

Experiments are conducted to examine the variation of recognition scores (for all types of overlapping) with the size of the training data. Therefore, for part 11, apart from the initial 60 samples (50 pure plus 10 overlapping), we use 70 samples (50 pure plus 20 overlapping), 80 samples (50 pure plus 30 overlapping), 90 samples (50 pure plus 40 overlapping), and 100 samples (50 pure plus 50 overlapping) of overlapping fingerprint images separately for training.

While testing, only the distorted versions of overlapping fingerprint images are used. The purpose is to investigate whether the classifiers can recognize the overlapping fingerprint classes even in the presence of distortions. As shown in Table 1, in each of the parts 1 to 10 of the experiment, 50 distorted fingerprint images belonging to the concerned type of overlapping are used for testing. However, in part 11, a total of 500 distorted fingerprint images, belonging to all the ten types of overlapping, are considered for testing the classifiers.



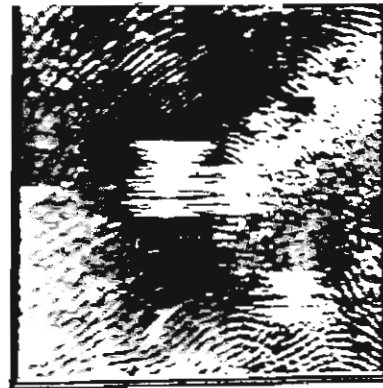
(a) 10% random noise



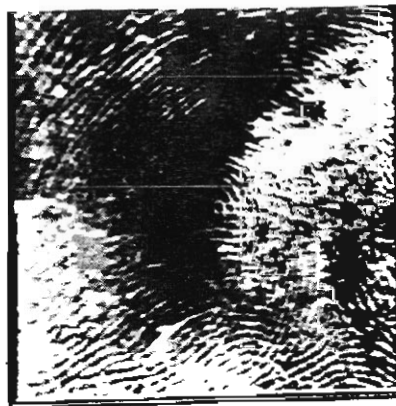
(b) cutmark (forward)



(c) information loss (black), i.e., smudging



(d) information loss (white), i.e., under inking



(e) averaging

Figure 4 - Different varieties of noise introduced into the overlapping fingerprint images

Note that the purpose here is to see whether the classifiers can identify any kind of distorted overlapping patterns, in contrast to parts 1 to 10 where only a particular type of overlapping is considered.

4.4 Results

The results obtained by the MLP are compared with those of the k -nearest neighbor (k -NN) classifier [15], with $k = 1, 3, 5$ and the Bayes' classifier.

Both the types of classifiers (MLP and k -NN) prove that the classes are well separable in the feature space selected here.

During the training of MLP, zero misclassification is obtained after 5000 iterations, for sixty training samples. The learning rate is initially considered to be 0.1. It is then changed after every 1000 iterations according to the schedule 0.05, 0.02, 0.01 and 0.001, respectively.

During the testing phase, distorted overlapping fingerprint images are used, as described in Sec. 4.3. Table 2 shows the overall performance of the test data in terms of percentage ranges (where the first and last figures denote the minimum and maximum values, respectively, of recognition scores obtained by MLP and k -NN with $k = 1$ and $k = 3$). The scores are obtained with various combinations (as described in Section 4.2) of 3, 4 or 5 fuzzy geometrical input features. As the recognition rates are poor with k -NN for $k = 5$ and Bayes' classifiers, these results are not included in the table. The best results (with all the classifiers used) are achieved with the combination of the three particular features *viz.*, height, length and IOAC. The other combinations of fuzzy geometrical features are not as effective in classifying the fingerprints. Incidentally, increasing the number of input features to 4 or 5 does not necessarily improve the performance of the classifiers, rather

they sometimes tend to confuse the learning and generalization

It is also seen that the greater the extent of overlapping, the better is its identification as an overlapping class. When the amount of overlapping is less, the classifiers tend to make the decision in favor of the background image (see Fig. 2 a).

The nature of variation of overall performance with different types of distortions for all the ten types of overlapping fingerprint images, using different classifiers, are found to be similar. To exemplify it, the performances of the various classifiers on the distorted fingerprints belonging to all the overlapping types (*i.e.*, part 11 of Table 1) are shown in Table 3. It is seen from the table that with all the classifiers used, the best results are obtained with MLP. The k -NN classifier, with $k = 1$, gives comparable results.

It is also observed from Table 3 that among the various artificial distortions, averaging (Section 4.1.4) hinders the recognition least, followed by cutmarks (both forward and reverse) and then smudging. Under inking, which introduces more white pixels, produces the worst results. These corroborate the findings of the earlier investigation [11] using fuzzy geometrical features.

Figure 5 shows, as an example, the variation (with the size of training data) of recognition scores of MLP and k -NN ($k = 1, 3$) for identifying all the types of overlapping fingerprints. Here the input features are considered to be the three fuzzy geometrical features *viz.*, height, length and IOAC. Improvement in score is seen to be relatively more for 3-NN rule, although its overall score is least among the three classifiers (as in the case of Table 3).

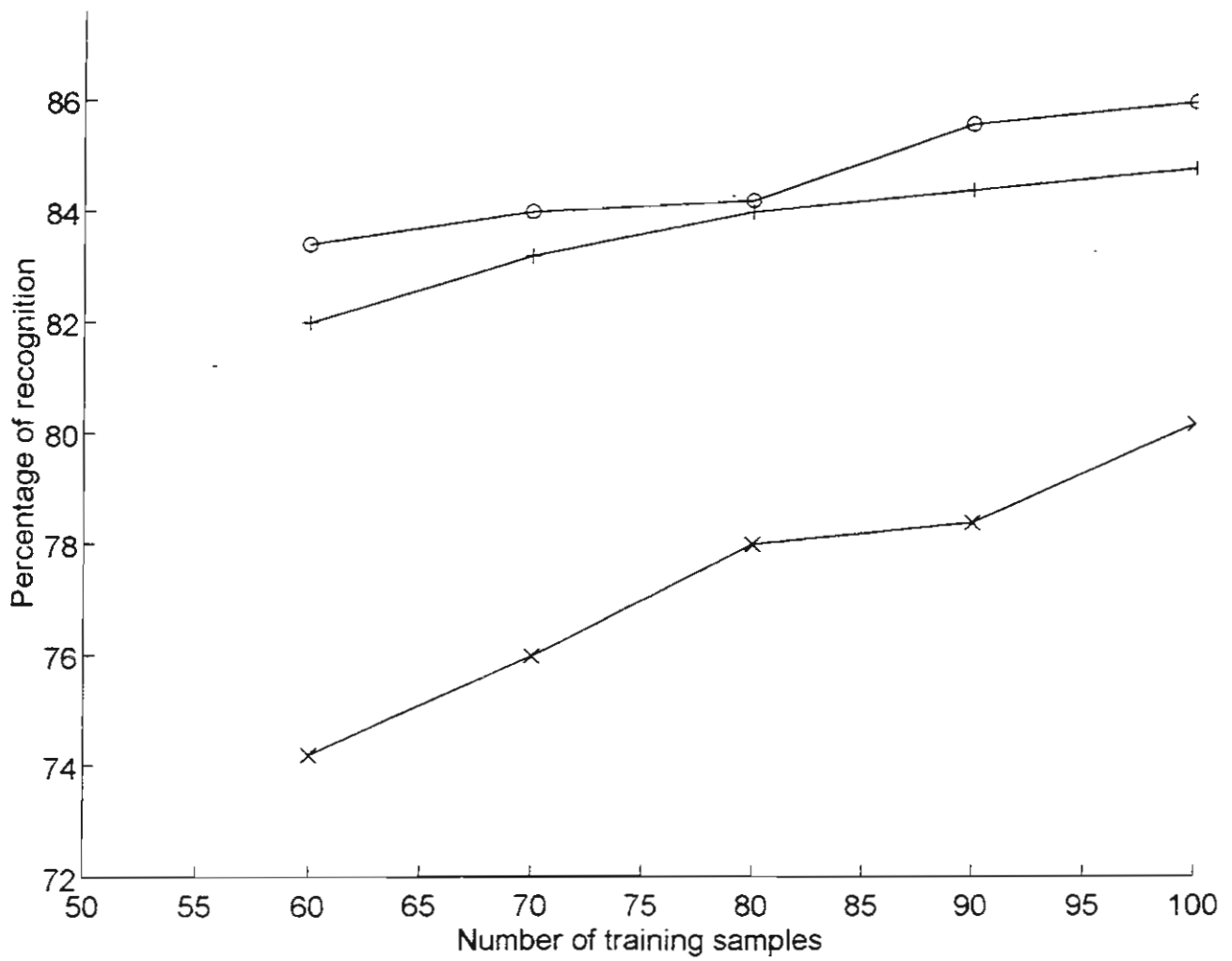


Figure 5 - Variation of Recognition Score with the number of the training samples

o : MLP; + : 1-NN; x : 3-NN

Table 1: Experimental design for training and testing the classifiers.

Part	Overlapping type	Training images	Test images
1	25% <i>y</i>	50 pure + 10 overlapping	50 corrupted images of this type of overlap
2	50% <i>y</i>	50 pure + 10 overlapping	50 corrupted images of this type of overlap
3	75% <i>y</i>	50 pure + 10 overlapping	50 corrupted images of this type of overlap
4	25% <i>x</i>	50 pure + 10 overlapping	50 corrupted images of this type of overlap
5	50% <i>x</i>	50 pure + 10 overlapping	50 corrupted images of this type of overlap
6	75% <i>x</i>	50 pure + 10 overlapping	50 corrupted images of this type of overlap
7	25% <i>x</i> + 25% <i>y</i>	50 pure + 10 overlapping	50 corrupted images of this type of overlap
8	50% <i>x</i> + 50% <i>y</i>	50 pure + 10 overlapping	50 corrupted images of this type of overlap
9	75% <i>x</i> + 75% <i>y</i>	50 pure + 10 overlapping	50 corrupted images of this type of overlap
10	100%	50 pure + 10 overlapping	50 corrupted images of this type of overlap
11	All 10 types combined	50 pure + 10 overlapping	500 corrupted images of all types of overlap

Table 2: Ranges of overall recognition scores (%), using MLP and k-NN with $k = 1, 3$, for various distorted overlapping patterns with different combinations of fuzzy geometrical features. H denotes height, L denotes length, I denotes IOAC, P denotes perimeter, C denotes compactness, W denotes width and B denotes breadth.

Overlapping type	H,L,I	P,C,I	W,B,I	H,L,W,B	H,L,P,C,I
25% <i>y</i>	56-80	36-68	52-76	56-78	54-78
50% <i>y</i>	60-80	48-64	56-60	60-70	54-70
75% <i>y</i>	62-82	44-72	50-70	56-76	52-74
25% <i>x</i>	52-82	40-68	40-60	42-70	50-70
50% <i>x</i>	62-90	46-66	54-80	58-82	56-80
75% <i>x</i>	50-84	44-72	40-60	46-80	46-72
25% <i>x</i> + 25% <i>y</i>	30-48	18-42	20-40	24-52	30-40
50% <i>x</i> + 50% <i>y</i>	50-74	24-60	30-50	32-60	42-64
75% <i>x</i> + 75% <i>y</i>	66-80	54-72	60-70	62-76	62-76
100%	74-84	60-76	70-80	72-82	70-82
All 10 types combined	74.2-83.4	60.6-74.4	72-80	75-82.4	72-82

Table 3: Recognition scores (%) with different classifiers for various types of distortions, on all ten types of overlapping taken together, with selective combinations of fuzzy geometrical features. H denotes height, L denotes length, I denotes IOAC. P denotes perimeter, C denotes compactness, W denotes width and B denotes breadth.

Features	Distortion type	Number of images	k-NN			MLP	Bayes'
			$k = 1$	$k = 3$	$k = 5$		
(H,L,I)	random	100	70	60	47	74	32
	cutmark	100	94	72	33	89	65
	smudging	100	82	77	59	83	81
	underinking	100	68	67	54	71	58
	averaging	100	96	95	62	100	84
	overall	500	82	74.2	51	83.4	64
(P,C,I)	random	100	21	25	13	56	20
	cutmark	100	76	71	52	75	61
	smudging	100	89	74	36	83	70
	underinking	100	53	51	39	58	54
	averaging	100	93	82	56	100	83
	overall	500	66.4	60.6	39.2	74.4	57.6
(W,B,I)	random	100	61	58	54	69	56
	cutmark	100	83	76	70	91	67
	smudging	100	76	75	70	76	70
	underinking	100	70	69	61	72	58
	averaging	100	87	82	69	92	65
	overall	500	75.4	72	64.8	80	63.2
(H,L,W,B)	random	100	67	59	42	73	33
	cutmark	100	88	82	57	88	62
	smudging	100	81	76	36	82	81
	underinking	100	73	71	45	78	52
	averaging	100	92	87	39	91	86
	overall	500	80.2	75	43.8	82.4	62.8
(H,L,P,C,I)	random	100	60	56	55	71	54
	cutmark	100	83	79	74	93	73
	smudging	100	75	73	68	79	65
	underinking	100	71	67	61	73	62
	averaging	100	88	85	82	94	80
	overall	500	77.4	72	68	82	66.8

5 Conclusions

The results of an investigation demonstrating the effectiveness of fuzzy geometrical features for identification of various distorted and noisy overlapping fingerprints are presented. The various distortions generated include random noise, cut-mark, smudging, under-inking and averaging. The classifiers considered are MLP, the k-NN classifier and the Bayes' classifier. An extensive comparison is made among them.

As expected, the lower the extent of overlapping (superimposition) of the fingerprints, the higher is the possibility of its being labeled by the classifiers as a member of the background image *i.e.*, as a member of a pure class. As the extent of overlapping increases, its chance of being identified as a member of the overlapping class increases.

Of all the fuzzy geometrical features, the combination of these three, *viz.*, height, length and IOAC (index of area coverage) are the best for distinguishing the various classes, even with distortions. Additional features or features in any other combination may sometimes confuse the classifiers.

The orientation of the overlapping, *i.e.*, whether in the x -axis or in the y -axis, does not significantly affect the recognition of overlapping patterns as a separate class. Finally, it has been noted that even in the presence of various forms of artificial distortions, the different classifiers can identify the five pure classes and the overlapping fingerprints fairly efficiently.

Improvement in recognition score with the number of training samples is seen to be more for 3-NN rule, although the overall performance is best for the MLP, followed by 1-NN rule.

Acknowledgments

This work is supported by a Project Grant (No. 22(235)/93/EMR-II) of the Council for Scientific and Industrial Research (CSIR), New Delhi, India. Dr. S. N. Sarbadhikari is a Research Associate in this project.

References

- [1] T. Ch Malleswara Rao, "Feature extraction for fingerprint classification," *Pattern Recognition*, vol. 8, pp. 181-192, 1976.
- [2] B. Moayer and K. S. Fu, "A syntactic approach to fingerprint pattern recognition," *Pattern Recognition*, vol. 7, pp. 1-23, 1975.
- [3] D. K. Isensor and S. G. Zaky, "Fingerprint identification using graph matching," *Pattern Recognition*, vol. 19, pp. 113-122, 1986.
- [4] K. Karu and A. K. Jain, "Fingerprint classification," *Pattern Recognition*, vol. 29, pp. 389-404, 1996.
- [5] D. E. Rumelhart and J. L. McClelland, eds., *Parallel Distributed Processing: Explorations in the Microstructures of Cognition*. Vol. 1, Cambridge, MA: MIT Press, 1986.
- [6] M. Kamijo, "Classifying fingerprint images using neural network : Deriving the classification state," in *Proceedings of IEEE International Joint Conference on Neural Networks*, (San Francisco, USA), pp. 1932-1937, 1993.
- [7] P. Baldi and Y. Chauvin, "Neural networks for fingerprint recognition," *Neural Computation*, vol. 5, pp. 402-418, 1993.
- [8] C. L. Wilson, G. T. Candela, and C. I. Watson, "Neural network fingerprint classification," *J. Artific. Neural Networks*, vol. 1, pp. 1-25, 1993.
- [9] S. K. Pal and A. Ghosh, "Fuzzy geometry in image analysis," *Fuzzy Sets and Systems*, vol. 48, pp. 23-40, 1992.
- [10] S. K. Pal and A. B. Leigh, "Motion frame analysis and scene abstraction: Discrimination ability of fuzziness measures," *J. Intelligent and Fuzzy Systems*, vol. 3, pp. 247-256, 1995.
- [11] S. K. Pal and S. Mitra, "Noisy fingerprint classification using multilayer perceptron with fuzzy geometrical and textural features," *Fuzzy Sets and Systems*, vol. 80, pp. 121-132, 1996.
- [12] S. Mitra, S. K. Pal, and M. K. Kundu, "Fingerprint classification using fuzzy multilayer perceptron," *Neural Computing and Applications*, vol. 2, pp. 227-233, 1994.
- [13] J. C. Bezdek and S. K. Pal, eds., *Fuzzy Models for Pattern Recognition*. New York: IEEE Press, 1992.
- [14] E. R. Henry, *Classification and uses of fingerprints*. London: George Routledge & Sons, 1900.
- [15] J. T. Tou and R. C. Gonzalez, *Pattern Recognition Principles*. London: Addison-Wesley, 1974.